

# Development of paclitaxel loaded pegylated gelatin targeted nanoparticles for improved treatment efficacy in non-small cell lung cancer (NSCLC): an *in vitro* and *in vivo* evaluation study

Minwei Gu<sup>1</sup>, Jun Luan<sup>3</sup>, Kun Song<sup>4</sup>, Cao Qiu<sup>4</sup>, XiaoLi Zhang<sup>4</sup> and Mingyong Zhang<sup>2</sup>✉

<sup>1</sup>Department of Thoracic, Affiliated Hospital of Jiang Nan University, WuXi214062, China; <sup>2</sup>Department of Thoracic Surgery, Qing Dao Municipal Hospital, Qing Dao, 266011, China; <sup>3</sup>Centre of Animal, Plant and Food testing, Nan Jing customs District P. R. China, Nan Jing, 210001, China; <sup>4</sup>Nanjing Hope Medical Laboratory Co., Ltd, Nan Jing, 210001, China

**Purpose:** To develop and evaluate paclitaxel (PTX) loaded pegylated gelatin targeted nanoparticles for improved efficacy in non-small cell lung cancer (NSCLC) treatment. **Method:** PTX loaded gelatin nanoparticles (PTX-GNP) were prepared by crosslinking with glutaraldehyde aqueous solution. These nanoparticles (NPs) were further incubated with PEG 400 to form PEGylated NPs (PEG-PTX-GNP). The NPs were evaluated for surface morphology, size, zeta potential, encapsulation efficiency, drug loading, *in vitro* drug release, cytotoxicity in an assay on cancer cell lines L132, *in vitro* cellular uptake in an assay in L132 and 293T cell lines, *in vivo* antitumor activity on female Balb/c mice, pulmonary deposition, histopathology, and immunohistochemical properties. **Results:** The nanoparticles were of spherical shape with smooth surface characteristics. The observed DL was of 20.18 to 32.11%, as particle size was of 90 to 115 nm. Zeta potential and polydispersity index (PDI) were within acceptable ranges. Encapsulation was effective when the NPs had a size of 80.50 nm to 98.12 nm. The PEGylated PTX loaded nanoparticles (PEG-PTX-GNP, GNP4) showed similar PTX release profile to that of the NP4 formulation. PEGylated NPs showed the desired PTX release pattern that is required for cancer treatment. In an *in vitro* cytotoxicity study, PEG-PTX-GNP showed the maximum antiproliferative activity over the period of 24 hours, followed by PTX-GNP, pure PTX and BPEG-GNP. PEG-PTX-GNP showed the highest internalization within both cell lines, followed by PTX-GNP and pure PTX. The survival rate of animals in PEG-PTX-GNP group was 100%, proving the safety and efficacy of the treatment. PEG-PTX-GNP showed the highest antitumor activity as compared to other formulations. The pulmonary deposition rate was the highest (6.5 to 12.55 µg/g) in PEG-PTX-GNP formulations. Histopathology and immunohistochemical study proved that PEG-PTX-GNP had greater anticancer potential than other tested formulations. **Conclusion:** This study confirms the potential use of paclitaxel loaded PEGylated gelatin targeted nanoparticles for improved efficacy in non-small cell lung cancer (NSCLC) treatment.

**Keywords:** antitumor, gelatin, nanoparticles, non-small cell lung cancer, Paclitaxel

**Received:** 21 July, 2020; revised: 05 April, 2021; accepted: 28 April, 2021; available on-line: 06 August, 2021

✉ e-mail: [mingyong2020@sina.com](mailto:mingyong2020@sina.com)

**Abbreviations:** EPR, enhanced permeation and retention; IPA, isopropyl alcohol; HCPT, 10-hydroxycamptothecin; NSCLC, non-small cell lung cancer; PEG, polyethylene glycol; PEG-PTX-GNP, PEGyla-

tion of PTX loaded gelatin nanoparticles; PTX, paclitaxel; PTX-GNP, PTX loaded gelatin nanoparticles; SCLC, small cell lung carcinoma

## INTRODUCTION

The lung cancer, also known as pulmonary carcinoma, is a malignant tumor characterized by uncontrolled growth of the cells in pulmonary tissues. Each year, nearly one million people are diagnosed with lung cancer worldwide and nearly 25% of deaths are caused by cancer, among which pulmonary cancer is the major cause of mortality (Kim *et al.*, 2012). Smoking, alcohol consumption, high fat diet and obesity are the main risk factors for the development of lung cancer in patients. The WHO has already given serious alarm regarding severe rise in mortality due to smoking and unhealthy diet in industrial countries (Torre *et al.*, 2016). The lung cancer is categorized in two main types: small cell lung carcinoma (SCLC) and non-small cell lung carcinoma (NSCLC). In one survey conducted in the USA it was found that among 220,000 lung patients, 85% of the early cases were NSCLC and the remaining were SCLC. In the current scenario, the available options for the treatment of NSCLC are chemotherapy, surgery, radiation therapy or combination of these (Pless *et al.*, 2015). In the advanced stage of NSCLC, chemotherapy is found ineffective or toxic to the patients. The remaining treatment options have a very low success rate and are systemically toxic due to non-specific effects, which kill normal cells (Garon *et al.*, 2015). The limitations of conventional drug delivery systems prompted the development of alternative approaches to overcome issues such as systemic toxicity. A combination of the anticancer drug with a natural bioactive molecule may be one of the solutions to reduce the side effects. Another approach is to use a nano size carrier system to increase the therapeutic concentration of a drug in a cancer cell due to enhanced permeation and retention (EPR). In addition to the microspheres, liposomes, and lipidic nanoparticles, the polymeric nanoparticles have been extensively used for targeted and controlled drug delivery. Among these systems, nanoparticles have gained prominent attention in the treatment of various types of cancer, including lung cancer. The surfaces of the nanoparticles can be decorated or modified to better target cancer cells that the immune system cannot identify. Nanoparticles can be easily distributed in the tumor area due to the excessive permeability of the tumor vasculature, lack of lymphatic drainage, and the EPR effect. The drug concentration in nanoparticulate form can be increased 10 to 100 times compared to the

free drug (Scott *et al.*, 2007; Ahmad *et al.*, 193; Peng *et al.*, 2009; Tahara *et al.*, 2017).

Many anti-cancer drugs have been studied in recent years, but most of them are hydrophobic and poorly soluble. Paclitaxel (PTX) is also a potent anti-cancer drug widely used in the treatment of NSCLC, but the clinical use of PTX is limited by high toxicity and low bio-availability due to poor solubility. Taxol is a preparation containing PTX used in the treatment of NSCLC, but it has been associated with various side effects such as cardiotoxicity, nephrotoxicity, neurotoxicity, and hypersensitivity. It has also been observed that PTX concentration in lung tissue is too low to elicit the therapeutic effect in treatment of the NSCLC. Thus, considering all these drawbacks of the current drug delivery system, there is a strong need to reduce side effects and increase the therapeutic efficacy of PTX (Su *et al.*, 2012; Shenb *et al.*, 2012; Goncalves *et al.*, 2001).

Gelatin is a naturally occurring protein biopolymer that is obtained from collagen under acidic or alkaline treatment. Having low antigenicity, it is widely used in parenteral formulations and approved as a plasma expander. In addition, gelatin has many advantages: it is biodegradable, biocompatible, non-toxic, water soluble, nonpyrogenic, inexpensive, can be easily sterilized, and has a higher content of amino acids such as glycine, proline, and alanine which stabilize the triple helical structure of gelatin (Tseng *et al.*, 2008). Gelatin can be easily chemically modified and conjugated due to the presence of ionizable groups such as amine, phenol, carboxyl, guanidine, and imidazole. Glutaraldehyde-crosslinked gelatin has greater stability, and increased circulation time in vivo compared to unmodified gelatin. All these properties make gelatin an ideal candidate for nanoparticulate drug delivery system (Karthikeyan *et al.*, 2013; Lu *et al.*, 2004).

Recently, particular attention has been paid to use of surface-modified gelatin nanoparticles in the treatment of cancer. Surface modification of gelatin nanoparticles with polyethylene glycol (PEG) has been widely used to prepare long circulating nanoparticles. PEGylated nanoparticles were shown to be less prone to degradation in calf serum than non-PEGylated nanoparticles (Hao *et al.*, 2012). It was also observed that the particle accumulation in tumor was nearly 6-fold higher for PEGylated nanoparticles, as compared to non-PEGylated nanoparticles (Schädlich A *et al.*, 2015). Doxorubicin-loaded PEGylated chitosan nanoparticles were found to be more efficient in inhibiting tumor growth than free doxorubicin and non-PEGylated doxorubicin-loaded nanoparticles (Scheeren *et al.* 2016). Another study showed that co-delivery of doxorubicin and paclitaxel in PEGylated

nanoparticles was more efficient in the treatment of non-small cell lung cancer than using non-PEGylated nanoparticles for drug delivery (Lv *et al.*, 2016). In a similar study, folic acid conjugated PEG nanoparticles were used for lung cancer targeting in mice model, where they showed enhanced cellular uptake of the nanoparticles confirmed by optical imaging due to receptor-mediated endocytosis (Yoo *et al.*, 2012). Another study developed PEGylated lipid nanocarriers to improve the anti-tumor activity of 10-hydroxycamptothecin (HCPT) in the treatment of lung cancer. An *in vivo* study showed that the developed PEGylated lipid nanoparticles had better efficacy against A549 lung cancer compared to the HCPT solution and non-PEGylated lipid nanocarriers (Zhang *et al.*, 2008). In this research, we developed surface-modified PEGylated PTX gelatin nanoparticles for the treatment of NSCLC that would reduce side effects, cytotoxicity, increase cellular uptake, and improve biodistribution in lung cancer tissue.

## MATERIALS AND METHODS

### Materials

Paclitaxel (PTX) was purchased from Baoji Guokang Bio-Technology Co., Ltd. (Baoji, Shaanxi, China); Gelatin Type-B, 175 g Bloom (from bovine skin) was purchased from Sigma-Aldrich (USA); Tween 80, sodium sulfate, isopropyl alcohol, glutaraldehyde (25%), sodium metabisulfite solution (12%), Sephadex G-50 column, and polyethylene glycol 400 (PEG 400) were purchased from Sigma-Aldrich USA.

**Cell culture and animals.** The NSCLC cell lines (293T and L132) for this study were obtained from the Shanghai Institute of Cell Biology. The cells were cultured in Roswell Park Memorial Institute 1640 (RPMI-1640) medium supplemented with 10% fetal bovine serum, 1% penicillin and 100 µg/ml streptomycin sulphate at 37°C in atmosphere of 5% CO<sub>2</sub>. BALB/c-nu/nu athymic mice were obtained from the Centre of Animal, Plant and Food Testing, Nan Jing customs District. P.R. China, Nan Jing, 210001, China. All animal experiments were conducted with accordance with institutional animal ethical committee of Centre of Animal, Plant and Food Testing, Nan Jing customs District. P.R. China, Nan Jing, 210001, China, with prior approval (ETHL/00432/CAPFT/2019/01)

**Preparation of PTX loaded gelatin nanoparticles.** PTX loaded gelatin nanoparticles were prepared using 175 g Bloom gelatin, which indicates the molecular weight of the gelatin polymer. Gelatin was dissolved in

**Table 1. Composition of PTX loaded gelatin nanoparticles (PTX-GNP)**

Sr. No	Ingredients	NP1	NP2	NP3	NP4
1	PTX (mg)	2	2	2	2
2	Gelatin (mg)	100	150	200	250
3	Tween 80 (mL)	5	10	15	20
4	20% Sodium sulfate aqs solution (mL)	1.5	1.5	2.0	2.0
5	Isopropyl alcohol (mL)	1	1	1	1
6	Double distilled water (mL)	q.s.	q.s.	q.s.	q.s.
7	20% Sodium sulfate aqs solution (mL)	5	5	6	6
8	20% Glutaraldehyde (mL)	0.5	0.5	1	1.5
9	1.5% sodium metabisulfite solution (mL)	4	4	5	5

water containing varying amount of Tween 80. This polymeric solution was heated at 40–45°C under continuous magnetic stirring at 400 rpm for 1 h. Next, 1.5 to 2 mL of 20% aqueous solution of sodium sulfate was added drop wise under continuous stirring. PTX was dissolved in isopropyl alcohol (IPA) at a concentration of 2 mg/mL and added to gelatin solution containing sodium sulfate, then 5 to 6 mL sodium sulfate solution was added with stirring until the solution became cloudy. The appearance of turbidity indicates the formation of gelatin aggregates. Next, nearly 1 mL double distilled water was added drop wise to the solution, until it became clear again. An aqueous solution of glutaraldehyde (20%) was then added to crosslink the gelatin. The crosslinking process was stopped by adding 4 to 5 mL of sodium metabisulfite solution (15%). The resulting solution was stirred for 1 h and the product was purified on Sephadex G-50 column (Amjadi *et al.*, 2019). The nanoparticles were lyophilized in a freeze dryer for 72 h and stored at –20°C. The composition of the formula is shown in Table 1.

**PEGylation of PTX loaded gelatin nanoparticles (PEG-PTX-GNP).** PEGylation of PTX-GNP was performed immediately after lyophilization of the nanoparticles. PTX-GNP were incubated with 1500 µg of PEG 400 (molecular weight 8000–10,000) per milligram nanoparticle and further diluted with PBS buffer to a final volume of 200 µL and incubated for 30 minutes at room temperature using rotary shaker (Amjadi *et al.*, 2019).

#### Statistical analysis

Statistical analysis was done using a SAS statistical kit (Version 9.0; SAS Institute, Inc., Cary NC). The differences were considered statistically significant at  $p < 0.05$ .

#### Characterization of PTX-GNP and PEG-PTX-GNP

**PTX entrapment efficiency in gelatin nanoparticles.** The PTX loaded nanoparticle suspension was centrifuged at 20,000 rpm for 30 min and the clear supernatant was separated by decantation. The amount of free (unloaded) drug was determined by injecting the supernatant liquid into an HPLC equipped with UV detector. The PTX entrapment efficiency in gelatin nanoparticles was calculated using the following equation (Hamarat *et al.*, 2016):

$$\% \text{ E.E of PTX} = \frac{\text{Total PTX} - \text{free PTX}}{\text{Total PTX amount}} \times 100$$

**PTX loading in gelatin nanoparticles.** Five milligrams of PTX loaded gelatin nanoparticles was added to hot water and shaken for 1 hour in a water bath shaker maintained at 40–45°C, to allow dissolving of the outer layer of gelatin. Nearly 15 ml of ethanol was added to the flask with dissolved gelatin. The flask was then shaken by hand for 15 minutes to extract the PTX in ethanol. The dispersion was then filtered through a 0.45 µm syringe filter. The filtrate containing PTX was determined by HPLC. The PTX loading was calculated according to the following formula (Hamarat *et al.*, 2016).

$$\% \text{ PTX loading} = \frac{\text{PTX Entrapped}}{\text{Weight of nanoparticles}} \times 100$$

**PTX release from gelatin nanoparticles.** PTX loaded gelatin nanoparticles (20 mg) were dispersed in 50 mL of pH 7.4 phosphate buffer and incubated at 37°C. Samples (2 mL) were taken at a predetermined time interval and replenished with fresh buffer solution (2 mL) to maintain the sinking conditions. The taken sample

was centrifuged for 20 minutes at 70,000 rpm using an ultracentrifuge. The nanoparticle-free supernatant was separated and extracted twice with 5 mL of ethanol. The extracted solution was filtered through a 0.45 µm syringe filter and used to estimate PTX release from nanoparticles using HPLC (Hamarat *et al.*, 2016).

**Particle size, Zeta potential polydispersity index (PDI) and yield of nanoparticles.** PTX loaded gelatin nanoparticles were dispersed in double distilled water (10 mL) and sonicated for 5 min in a water bath sonicator. The nanoparticle suspension was diluted 10 times with double distilled water and a drop of suspension was mounted on foil paper, dried coated with gold and examined under scanning electron microscopy (SEM) (Leo 435 VP, Cambridge, UK.) at an operating distance of 8–8.5 mm and accelerating voltage of 15.0 kV. Particle size, PDI and zeta potential of diluted nanoparticles were measured using Zetasizer (Malvern instruments DTS Ver 4.10). The yield of nanoparticles was calculated from the weight of freeze dried PTX loaded gelatin nanoparticles.

**Cytotoxicity assay study.** Cytotoxicity of the nanoparticle formulations was determined in L132 cancer cell line with a 3-(4,5-dimethylthiazol-2-yl)-2,5 diphenyl tetrazolium bromide assay. The cells were grown in 96 well tissue culture plate at  $1 \times 10^5$  per well. The cells were treated either with PTX loaded gelatin nanoparticles (PTX-GNP), PTX loaded PEGylated gelatin nanoparticles (PEG-PTX-GNP), pure PTX or blank PEGylated gelatin nanoparticles (BPEG-GNP) at concentrations of 0.5 mg/mL and 0.75 mg/mL for 48 hours. 3-(4,5-dimethylthiazol-2-yl)-2,5 diphenyl tetrazolium bromide stock solution was added to each culture at 10% of the final culture volume and the cells were incubated for 4 hours at 37°C. Then, the medium was collected, and centrifuged, and dimethyl sulfoxide was added to it to dissolve the formazan crystals. The absorbance of the medium was measured at 490 nm using microplate reader. The cytotoxicity was calculated as the percentage of viability in each well (Singh *et al.*, 2008).

**In vitro cellular uptake assay in L132 and 293T cell lines.** A cellular uptake assay was used to determine the accumulation of PTX released from nanoparticles in the cell line. L132 and 293T cell lines were seeded in 12 well culture plates at a density of  $10^5$  cells/well and incubated for 24 h. Incubated cell lines were treated with either PTX-GNP, PEG-PTX-GNP or pure PTX at concentrations of 0.03, 0.06 and 1.0 µM for 8 h. After incubation, the cells were trypsinized and washed with saline buffer three times. The cells were centrifuged, and the cell mass was treated with lysis buffer and sonicated. The resulting solution was analyzed with HPLC to determine the internal accumulation of the drug in the cell lines (Liu *et al.*, 2011).

**In vivo antitumor activity.** *In vivo* antitumor activity of PTX-GNP, PEG-PTX-GNP and pure PTX was studied in 8- to 10-week-old female Balb/c mice. Each of the animals was anesthetized with isoflurane and had its left flank shaved and their left lung injected at a depth of 4 mm with approximately 1.4 million L132 cells in exponential growth phase. The animals were kept under observation (nearly 24 days) until the palpable tumors formed. The animals were divided in to four groups as follows: 1) PTX-GNP treated 2) PEG-PTX-GNP treated 3) pure PTX treated 4) no treatment or control group. All formulations were administered by inhalation to each group of animals at a dose of 3 mg/kg for 3 days using nasal insufflators. The experiment was continued until the established end points, at which the volume and weight of the tumors were measured to determine the

**Table 2. Physical characterization of nanoparticles**

Type of NP	PTX loaded gelatin NP (PT-GNP)			
Batch Code	NP1	NP2	NP3	NP4
Particle size	90.44 nm	96.50 nm	101.59 nm	110.525 nm
PDI	0.125	0.135	0.234	0.298
Zeta potential	19.12±5.5	20.20±2.5	21.25±2.5	22.25±3.0
Type of NP	PEGylated PTX-loaded gelatin NP (PEG-PTX-GNP)			
Batch Code	GNP1	GNP2	GNP3	GNP4
Particle size	93.24 nm	97.99 nm	103.5 nm	112.50 nm
PDI	0.130	0.143	0.250	0.30
Zeta potential	20.10±3.5	20.25±2.3	21.30±4.5	22.30±3.5

antitumor activity of investigated treatment (Long *et al.*, 2014).

**Pulmonary deposition study.** The amount of PTX deposited in the lungs of PTX-GNP-, PEG-PTX-GNP- or pure PTX-treated animals was assessed at 1, 3, 12 and 24 h post treatment. The animals were sacrificed, and their lungs were carefully removed, washed thrice with pH 7.4 phosphate buffer and soaked in nitric acid solution (70%) for 20 h. The digested and homogenized lungs were centrifuged and the supernatant was HPLC-analyzed to determine the PTX content (Long *et al.*, 2014).

**Histopathology study.** Histopathology study was performed on separated cancer tissues from animals. The tumors were cut in to 30 µm sections, deparaffinized and rehydrated with eosin and hematoxylin. Slides were viewed under a light microscope and pictures were taken (Li *et al.*, 2017).

**Immunohistochemical study.** The tumor samples were collected and immediately put in 4% buffered paraformaldehyde for 12 hours. The samples were then rehydrated with alcohol gradient and embedded in paraffin. The paraffin blocks were sliced into 5 µm sections and mounted on poly-l-lysine-coated slides. Next, deparaffinized tumor sections were rehydrated with 3% hydrogen peroxide and alcohol and incubated for 30 min with capase-3 and MMP-9 antibodies and stained (Li *et al.*, 2017).

## RESULTS AND DISCUSSION

### Preparation of PEGylated, PTX-loaded gelatin nanoparticles (PEG-PTX-GNP)

PEGylated PTX-loaded gelatin nanoparticles were produced in two steps: 1) synthesis of PTX loaded gelatin nanoparticles followed by 2) PEGylation of PTX loaded gelatin nanoparticles. PEGylation of nanoparticles is widely recommended for enhanced biocompatibility, non-immunogenicity, nontoxicity, and low protein adsorption. PEGylation also increases the blood circulation time and cellular uptake of the nanoparticles. The

surface characteristics of nanoparticles (PTX-GNP) were examined using FESEM. The nanoparticles had a spherical shape with a smooth surface (Fig. 1). In dry form, the nanoparticles were separated from each other and had free flowing properties. The PEGylation of nanoparticles (PEG-PTX-GNP) did not affect their surface characteristics.

The size, zeta potential and PDI are important factors in determining the stability and performance of an NP. The NP size between 60 and 200 nm is considered suitable for cancer therapy as it enhances the EPR effect in passive targeting. Up to 80% of aerosol particles measuring less than 1 µm in diameter can be easily exhaled after inspiration, without being deposited. Particles smaller than 100 nm can effectively deposit in alveolar region leading to improved chemotherapy outcomes for sensitive and resistant non-small cell lung cancer (Mehrotra *et al.*, 2011). Both PTX-GNP and PEG-PTX-GNP NP are of appropriate size to protect against RES by avoiding endocytosis and destruction. Zeta potential values between -30 mV and +30 mV are considered ideal for achieving better physical stability of the nanoparticle dispersion and suspension. Both PT-GNP and PEG-PTX-GNP had ideal zeta potential values to maintain their stability (Du *et al.*, 2009). PDI of both types of nanoparticles were also found within acceptable range (less than 0.3), which indicated homogeneous dispersion of the NPs. The narrow PDI of nanoparticles may be due to the presence of PEG chains that prevent nanoparticle aggregation. Overall, the prepared nanoparticles had improved stability, PDI, zeta potential and particle size. Table 2 shows all physical parameters of the NPs.

The EE of PTX in nanoparticles was determined by calculating the free (non-entrapped) drug content in supernatant using HPLC. The EE of all formulations was between 80.50 and 98.12%. A direct relationship was observed between the concentration of gelatin and EE. In this study, we have used gelatin Type-B, 175 g Bloom. Gelatin, due to its gelling and sticky properties, has sufficient strength to hold the drug inside the nanoparticles, which increased the EE and DL of PTX (Karthikeyan *et al.*, 2013). The observed DL within nanoparticle for-

**Table 3. PTX entrapment efficiency and loading in gelatin nanoparticles**

Type of NP	PTX loaded gelatin NP (PT-GNP)			
Batch Code	NP1	NP2	NP3	NP4
% EE	80.50 nm	82.90 nm	97.89 nm	98.12 nm
% DL	20.18	27.12	30.17	32.11
% Yield	78.20	82.25	90.25	95.12

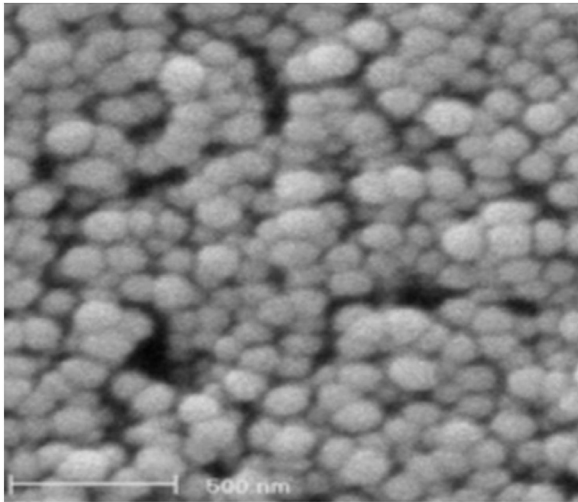


**Figure 1.** Surface morphology of PEGylated NPs showing spherical and smooth surface characteristics

mulations was between 20.18 and 32.11%. The yield of NPs ranged from 78.20% to 95.12% and increased with increasing concentration of gelatin. Table 3 shows comparative EE, DL and yield of NP's.

#### PTX release from PTX-GNP and PEG-PTX-GNP

*In vitro* PTX release from PTX-GNP and PEG-PTX-GNP was studied in pH 7.4 saline phosphate buffer. NP4 formulation showed initial burst release of 20.13% from PTX-GNP nanoparticles followed by a sustained release of almost 67% over a period of 40 hours. The slow and gradual release was observed due to the greater amount of gelatin used in the nanoparticle preparation as compared to other formulations such as NP1, NP2 and NP3. Formulations containing lower amount of gelatin did not show satisfactory PTX release profile as shown in Fig. 2.

The PEGylated PTX-loaded nanoparticles (PEG-PTX-GNP, GNP4) showed similar PTX release profile to that of NP4 formulation (Fig. 2). This observation clearly indicated that PEGylation of nanoparticles did not alter the release characteristics of the pure PTX loaded gelatin nanoparticles. Sustained and gradual release of a drug is always a desirable feature in cancer treatment to provide a longer duration of therapeutic action. PEGylated NPs

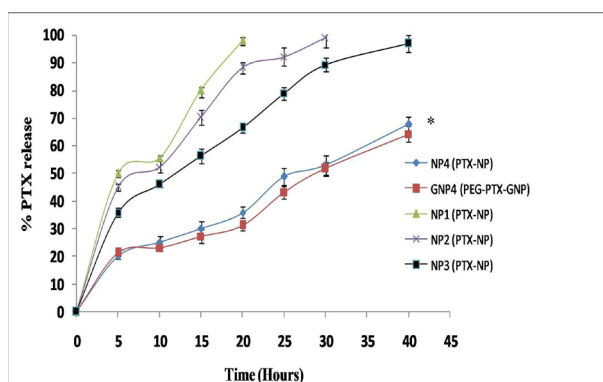


**Figure 2.** Comparative *in vitro* PTX release profile from PEGylated and non-PEGylated NPs in pH 7.4 saline phosphate buffer. The nanoparticulate formulation showed a sustained release behavior and the release was significantly prolonged ( $*P < 0.05$ .) Data presentation of mean S.D. of  $\pm 0.5$ .

showed a desired PTX release pattern that is required for the cancer treatment.

#### Cytotoxicity assay study

The cytotoxicity of pure PTX, blank PEGylated gelatin nanoparticles (BPEG-GNP), PTX-GNP and PEG-PTX-GNP were determined in the human SCLC cell line L132. All formulations were incubated with the cells for the period of 24 hours at two different concentrations. Cytotoxicity was calculated based on cell viability. Among all these formulations, PEG-PTX-GNP showed the maximum antiproliferative activity (i.e., cytotoxicity) over the period of 24 hours, followed by PTX-GNP, pure PTX and BPEG-GNP. The cytotoxicity was concentration dependent i.e., the higher the concentration, the higher the cytotoxicity. PEG-PTX-GNP (30%, 25.5% cell viability) showed nearly two-fold increase in cytotoxicity as compared to PTX-GNP (55.9%, 50.6% cell viability), as shown in Fig. 3.

PTX interferes with microtubule growth, which destroys the cell's cytoskeleton and shows the antitumor activity (Tran *et al.*, 2014). In our experiments, pure PTX showed cytotoxic activity when compared to blank PEGylated gelatin nanoparticles (BPEG-GNP). After phagocytosis or endocytosis, the nanoparticles reach the acidic lysosomes, and if they contain the drug, its release takes place in a sustained and gradual manner.

#### *In vitro* cellular uptake assay in L132 and 293T cell lines

Cellular uptake assay was conducted in L132 and 293T cell lines over the period of 12 h at various NP concentrations, ranging from 0.03 to 1.0  $\mu\text{M}$ . A linear correlation was observed between the NPs' concentration and cellular uptake in both cell lines. In both cell lines, PEG-PTX-GNP showed the highest internalization, followed by PTX-GNP and pure PTX. PEG-PTX-GNP showed nearly two-fold higher cellular uptake as compared to PTX-GNP, as shown in Fig. 4.

The PEGylation of nanoparticles protects them from opsonization, surface aggregation, and phagocytosis, and prolongs their systemic circulation. It also increases PER effect for the long circulating NPs, providing unique opportunities for interaction with cell surfaces (Babu *et al.*, 2013). These advantages of NPs' PEGylation increase

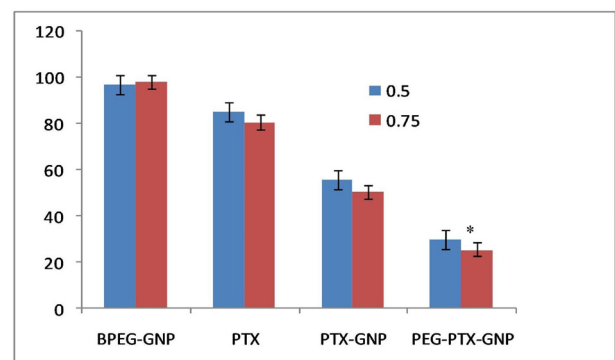


**Figure 3.** Comparative cytotoxicity of blank PEGylated gelatin NPs (BPEG-GNP), pure PTX (PTX), PTX-loaded gelatin NPs (PTX-GNP) and PEGylated gelatin PTX-loaded NPs (PEG-PTX-GNP) in L132 human lung cancer cell line at 0.5 and 0.75 mg/mL.

All formulations showed concentration dependent cytotoxicity and PEG-PTX-GNP showed minimum cytotoxicity i.e., maximum antiproliferative effect on cell line ( $*P < 0.05$ ). The significance between the various formulations was evaluated using SAS software.  $*P < 0.05$ . Data presentation of mean S.D. of  $\pm 1.5$

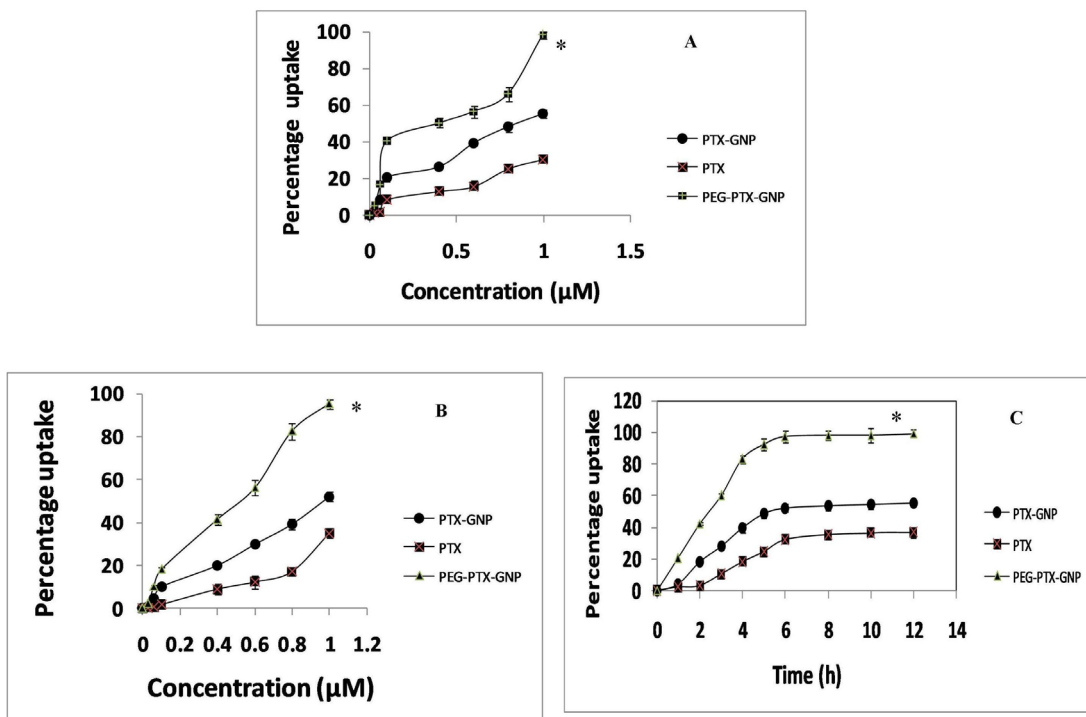


Figure 4. Comparative *in vitro* cellular uptake studies of pure PTX (PTX), PTX-loaded gelatin NPs (PTX-GNP) and PEGylated gelatin PTX-loaded NPs (PEG-PTX-GNP) in L132 cell line (A); in 293T cell line (B); averaged for both cell lines (C).

The significance of the difference between the various formulations was evaluated using SAS software. \* $P < 0.05$ . (\*The results obtained in this study are statistically significant). Data presentation of mean S.D. of  $\pm 0.5$

the cellular uptake of PEG-PTX-GNP when compared to PTX-GNP or pure PTX. The cellular uptake was found to be time dependent in all types of formulations in both types of cells. However, the saturation of cel-

lular uptake was observed after 6 h of incubation with nanoparticles.

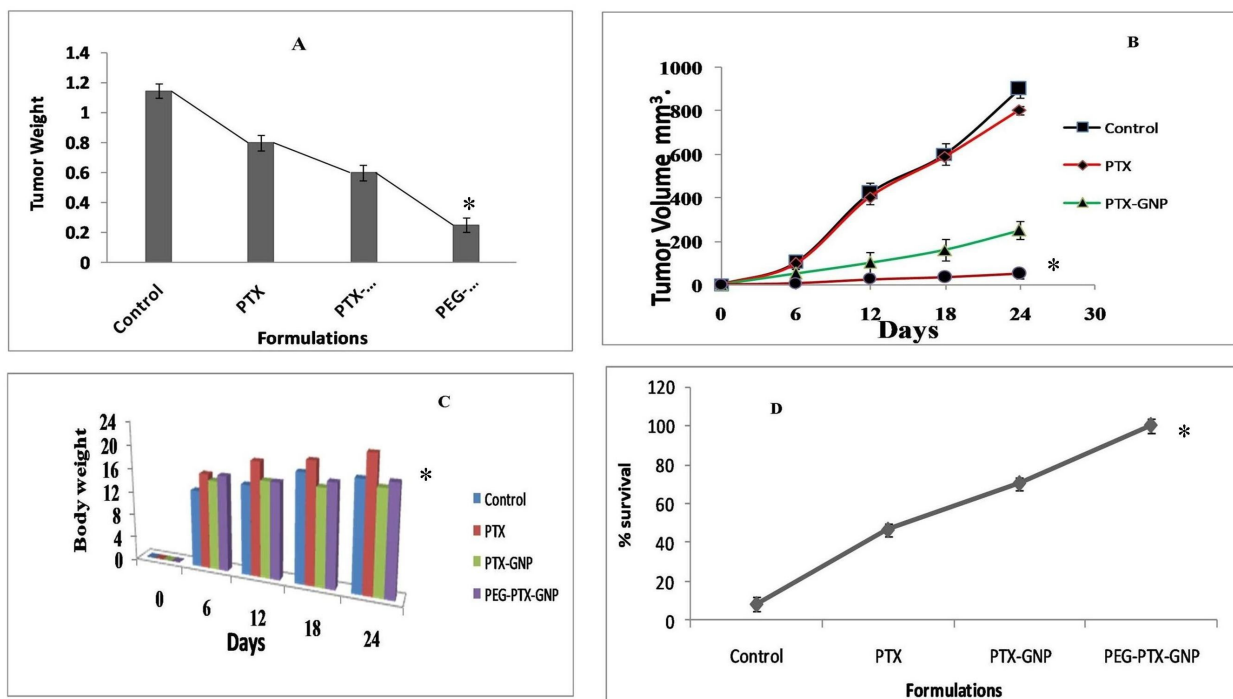


Figure 5. Tumor weight (A) and volume (B) suppression after treatment with formulations; Body weight (C) and survival rate (D) after treatment with formulations.

The significance of the differences between the various formulations was evaluated using SAS software. \* $P < 0.05$ . (\*The results obtained in this study are statistically significant). Data presentation of mean S.D. of  $\pm 0.5$

### In vivo antitumor activity

Antitumor activity of the NPs was determined based on the measurements of tumor volume, tumor weight, body weight and survival rate of the BALB/c-nu/nu athymic mice injected with L132 tumor cells. As shown in Fig. 5A, the smallest tumor in terms of weight (0.25 g) was observed in animals treated with PEG-PTX-GNP, followed by PTX-GNP (0.6 g), PTX (0.8 g) and the control group, which showed the largest tumor weight of 1.15 g. The smallest tumor growth in animals indicates the maximum antitumor activity of the drug and can be attributed to the higher internalization and accumulation of NPs in tumor tissue.

The control group showed the highest tumor volume (nearly 900 mm<sup>3</sup>), while the PEG-PTX-GNP treated group's mean tumor volume was a mere 50 mm<sup>3</sup> and PTX-GNP treated group tumor volume was 250 mm<sup>3</sup> as shown in Fig. 5B.

The PEG-PTX-GNP treated group showed nearly 18-fold tumor suppression growth over the period of 24 days, as compared to the control group. This long-lasting tumor suppression was attributed to slow and gradual release of PTX from the PEGylated gelatin nanoparticles and enhanced cellular uptake and drug internalization in cancer tissue. In neither of the treated groups a reduction in body weight was observed, indicating that the administered PTX dose was well acceptable and tolerated (Fig. 5C).

The sustained and gradual PTX release from the NPs prevented accumulation and harm to the normal (non-cancer) cells. 24 days post-injection, the survival rate of animals in PEG-PTX-GNP treated group was a 100%, proving the safety and efficacy of the formulation. The control group showed the lowest survival rate of just 8.5% at the end of study (Fig. 5 D). Overall, PEG-PTX-GNP showed the excellent antitumor activity.

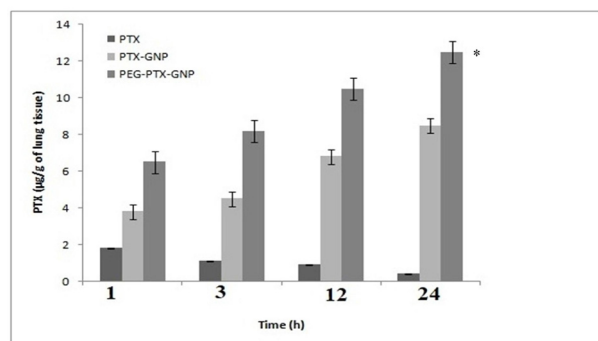


**Figure 6. Pulmonary deposition of PTX at various time points.** In case of PTX-GNP, the pulmonary deposition was increased from 3.8 µg/g to 8.5 µg/g over 24 h post-treatment. The pulmonary deposition rate was highest (6.5 to 12.55 µg/g) for the PEG-PTX-GNP formulations (\* $P < 0.05$ ). The significance between the various formulations was evaluated using SAS software. Data presentation of mean S.D. of  $\pm 0.5$

### Pulmonary deposition study

The pulmonary deposition of PTX was determined in the animals treated with pure PTX, PTX-GNP or PEG-PTX-GNP. The mice were sacrificed at 1, 3, 12 and 24 h post-treatment. The maximum deposition associated with pure PTX was 1.85 µg/g after 1 hour, but later no increase in deposition was observed. Instead, pure PTX showed decline in pulmonary deposition over time. But in case of PTX-GNP and PEG-PTX-GNP formulations, a gradual increase in pulmonary deposition was observed over time. In case of PTX-GNP, the pulmonary deposition was increased from 3.8 µg/g to 8.5 µg/g within the period of 24 hours. The pulmonary deposition rate was the highest (6.5 to 12.55 µg/g) for the PEG-PTX-GNP formulations (see Fig. 6). Maximum pulmonary deposition of PTX is desired for the best therapeutic effect for

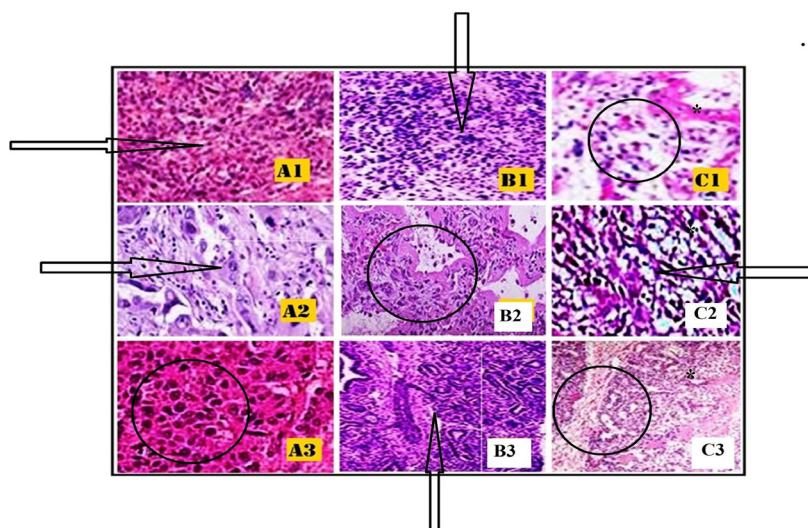


**Figure 7. Histopathology and Immunohistochemical analysis:**

(A1): Histopathology of tumor sections using hematoxylin stain obtained from control mice (Denser mass observed control A1 group shown by arrow); (A2): Histopathology of tumor sections using hematoxylin stain obtained from control mice (Denser mass observed in control group A2 shown by arrow); (A3): Histopathology of tumor sections using hematoxylin stain obtained from control mice (Denser mass observed in control group A3 shown by circle); (B1): Histopathology of tumor sections using eosin stain obtained from mice treated with PTX-GNP (Missing of denser and crowded mass shown by arrow); (B2): Histopathology of tumor sections using eosin stain obtained from mice treated with PTX-GNP (Missing of denser and crowded mass shown by circle); (B3): Histopathology of tumor sections using eosin stain obtained from mice treated with PTX-GNP (Missing of denser and crowded mass shown by arrow); (C1): Immunohistochemical analysis of cleaved caspase 3 from tumor section collected from mice treated with PEG-PTX-GNP (Missing of denser and crowded mass shown by circle); (C2): Immunohistochemical analysis of cleaved caspase 3 from tumor section collected from mice treated with PEG-PTX-GNP (Missing of denser and crowded mass shown by circle); (C3): Immunohistochemical analysis of cleaved caspase 3 from tumor section collected from mice treated with PEG-PTX-GNP (Missing of denser and crowded mass shown by circle). The significance between the various formulations was evaluated using SAS software. (\* $P < 0.05$ ).

the treatment of NSCLC. The continuous increase in pulmonary deposition of PEG-PTX-GNP over time was the result of PEGylation and smaller particle size of the formulations (Sukumar *et al.*, 2013).

### Histopathology and immunohistochemistry of the tumor

A dense and crowded extracellular mass was observed in the tumors from the control animals, while it was missing in animals treated with either PTX-GNP or PEG-PTX-GNP formulations, which indicated the anticancer potential of the formulations (Fig. 7A).

The immunohistochemical analysis also confirmed the antitumor potential of the PTX-GNP and PEG-PTX-GNP formulations. The highest caspase-3 levels were observed in the tumor specimens from the PEG-PTX-GNP-treated animals. Lower caspase-3 levels were observed in PTX-GNP-treated group. These observations indicate a greater anticancer potential of PEG-PTX-GNP. Conversely, MMP-9 expression was significantly reduced in animals treated with PEG-PTX-GNP as compared to PTX-GNP treatment group. Therefore, it could be concluded that PEG-PTX-GNP had greater anticancer potential than other tested formulations. We propose that it was due to the PEGylation of NPs, which increased cellular uptake and internalization in cancer tissue.

### CONCLUSION

The PEGylated NPs showed a gradual and slow-release profile upon systemic administration, enhanced encapsulation efficiencies, lower particle size, significant cytotoxicity in L132 and 293T cell lines and an increased pulmonary tissue deposition and antitumor activity and lesser cytotoxicity than non-PEGylated NPs. This study supports the potential use of paclitaxel loaded PEGylated gelatin targeted nanoparticles for improved efficacy in non-small cell lung cancer (NSCLC).

### Declaration of Conflict

The authors declare no conflict of interest for the presented manuscript.

### Funding statement

This research was funded by Nanjing Hope Medical Laboratory Co., Ltd (NO: 2020HP1070).

### REFERENCES

- Ahmad I, Longenecker M, Samuel J, Allen TM (1993) Antibody-targeted delivery of doxorubicin entrapped in sterically stabilized liposomes can eradicate lung cancer in mice. *Cancer Res* **53**: 1484–1488
- Amjadi S, Hamishehkar H, Ghorbani M (2019) A novel smart PEGylated gelatin nanoparticle for co-delivery of doxorubicin and betanin: A strategy for enhancing the therapeutic efficacy of chemotherapy. *Mat Sci Engin C* **97**: 833–841. <https://doi.org/10.1016/j.msec.2018.12.104>
- Babu A, Templeton AK, Munshi A, Ramesh R (2013). Nanoparticle-based drug delivery for therapy of lung cancer: progress and challenges. *J Nanomat* **1**: 1–11. <https://doi.org/10.1155/2013/863951>
- Du WL, Niu SS, Xu YL, Xu ZR, Fan CL (2009). Antibacterial activity of chitosan tripolyphosphate nanoparticles loaded with various metal ions. *Carbohydr Poly* **75**: 385–389. <https://doi.org/10.1016/j.carbpol.2008.07.039>
- Garon EB, Rizvi NA, Hui R (2015) Pembrolizumab for the treatment of non-small-cell lung cancer. *New Engl J Med* **372**: 2018–2028. <https://doi.org/10.1056/NEJMoa1501824>
- Goncalves A, Braguer D, Kamath K, Martello L, Briand C, Horwitz S, Wilson L, Jordan MA (2001) Resistance to Taxol in lung cancer cells associated with increased microtubule dynamics. *Proc Natl Acad Sci* **98**: 11737–11742. <https://doi.org/10.1073/pnas.191388598>
- Hamarat Sanlier S, Yasa M, Cihnioglu AO, Abdulhayoglu M, Yilmaz H, Ak G (2016) Development of gemcitabine-adsorbed magnetic gelatin nanoparticles for targeted drug delivery in lung cancer. *Art Cells Nanomed Biotechnol* **44**: 943–949. <https://doi.org/10.3109/21691401.2014.1001493>
- Hao N, Liu H, Li L, Chen D, Li L, Tang F. (2012) In vitro degradation behavior of silica nanoparticles under physiological conditions. *J Nanosci Nanotechnol* **12**: 6346–6354. <https://doi.org/10.1166/jnn.2012.6199>
- Karthikeyan S, Prasad NR, Ganamani A, Balamurugan E (2013) Anticancer activity of resveratrol-loaded gelatin nanoparticles on NCI-H460 non-small cell lung cancer cells. *Biomed Prevent Nutr* **3**: 64–73. <https://doi.org/10.1016/j.bionut.2012.10.009>
- Kim I, Byeon HJ, Kim TH (2012) Doxorubicin-loaded highly porous large PLGA microparticles as a sustained-release inhalation system for the treatment of metastatic lung cancer. *Biomaterials* **33**: 5574–5583. <https://doi.org/10.1016/j.biomaterials.2012.04.018>
- Li K, Liang N, Yang H, Liu H, Li S (2017) Temozolomide encapsulated and folic acid decorated chitosan nanoparticles for lung tumor targeting: improving therapeutic efficacy both *in vitro* and *in vivo*. *Oncotarget* **8**: 111318. <https://doi.org/10.18632/oncotarget.22791>
- Liu J, Liu J, Chu L, Wang Y, Duan Y, Peng L, Yang C, Wang L, Kong D (2011) Novel peptide-dendrimer conjugates as drug carriers for targeting non-small cell lung cancer. *Int J Nanomed* **6**: 59–69. <https://doi.org/10.2147/IJN.S14601>
- Long JT, Cheang TY, Zhuo SY, Zeng RF, Dai QS, Li HP, Fang S (2014) Anticancer drug-loaded multifunctional nanoparticles to enhance the chemotherapeutic efficacy in lung cancer metastasis. *J Nanobiotechnol* **12**: 1–11. <https://doi.org/10.1186/s12951-014-0037-5>
- Lu Z, Yeh TK, Tsai M, Au JL, Wientjes MG (2004) Paclitaxel-loaded gelatin nanoparticles for intravesical bladder cancer therapy. *Clin Cancer Res* **10**: 7677–7684. <https://doi.org/10.1158/1078-0432.CCR-04-1443>
- Lv S, Tang Z, Li M (2014) Co-delivery of doxorubicin and paclitaxel by PEG-polypeptide nano vehicle for the treatment of non-small cell lung cancer. *Biomaterials* **35**: 6118–6129. <https://doi.org/10.1016/j.biomaterials.2014.04.034>
- Mehrotra A, Nagarwal RC, Pandit JK (2011) Lomustine loaded chitosan nanoparticles: characterization and *in-vitro* cytotoxicity on human lung cancer cell line L132. *Chem Pharm Bull* **59**: 315–320. <https://doi.org/10.1248/cpb.59.315>
- Peng G, Tisch U, Adams O (2009) Diagnosing lung cancer in exhaled breath using gold nanoparticles. *Nat Nanotechnol* **4**: 669–673. <https://doi.org/10.1038/nnano.2009.235>
- Pless M, Stupp R, Ris HB (2015) Induction chemo radiation in stage IIIA/N2 non-small-cell lung cancer: a phase 3 randomised trial. *Lancet* **386**: 1049–1056. [https://doi.org/10.1016/S0140-6736\(15\)60294-X](https://doi.org/10.1016/S0140-6736(15)60294-X)
- Schädlich A, Caysa H, Mueller T, Tenambergen F, Rose C, Göpferich A, Kuntsche J, Mäder K (2015) Tumor accumulation of NIR fluorescent PEG-PLA nanoparticles: Impact of particle size and human xenograft tumor model. *ACS Nano* **5**: 8710–8720. <https://doi.org/10.1021/nn2026353>
- Scheeren LE, Nogueira DR, Macedo LB, Vinardell MP, Mitjans M, Infante MR, Rolim CM (2016) PEGylated and poloxamer-modified chitosan nanoparticles incorporating a lysine-based surfactant for pH-triggered doxorubicin release. *Colloids and Surfaces B: Biointerfaces* **138**: 117–127
- Scott WJ, Howington J, Feigenberg S (2007) Treatment of non-small cell lung cancer stage I and stage II: ACCP evidence-based clinical practice guidelines. *Chest* **132**: 234S–2342S. <https://doi.org/10.1378/chest.07-1378>
- Shen J, Yin Q, Chen L, Zhang Z, Li Y (2012) Co-delivery of paclitaxel and survivin shRNA by pluronic P85-PEI/TPGS complex nanoparticles to overcome drug resistance in lung cancer. *Biomaterials* **33**: 8613–8624. <https://doi.org/10.1016/j.biomaterials>
- Singh P, Gupta U, Asthana A, Jain NK (2008) Folate and folate-PEG-PAMAM Dendrimers: synthesis, characterization, and targeted anticancer drug delivery potential in tumor bearing mice. *Bioconjugate Chem* **19**: 2239–2252. <https://doi.org/10.1021/bc800125u>
- Su WP, Cheng FY, Shieh DB, Yeh CS, Su WC (2012) PLGA nanoparticles codeliver paclitaxel and Stat3 siRNA to overcome cellular resistance in lung cancer cells. *Int J Nanomed* **7**: 4269. <https://doi.org/10.2147/IJN.S33666>
- Sukumar UK, Bhushan B, Dubey P, Matai I, Sachdev A, Packirisamy G (2013). Emerging applications of nanoparticles for lung cancer diagnosis and therapy. *Int Nano Lett* **3**: 45. <https://doi.org/10.1186/2228-5326-3-45>
- Tahara Y, Yoshikawa T, Sato H (2017) Encapsulation of a nitric oxide donor into a liposome to boost the enhanced permeation and retention (EPR) effect. *Med Chem Comm* **8**: 415–421. <https://doi.org/10.1039/C6MD00614K>
- Torre LA, Siegel RL, Jemal A (2016) Lung cancer statistics. Lung cancer and personalized medicine. pp 1–19. Springer Cham

- Tran PH, Tran TT, Lee BJ (2014) Biodistribution and pharmacokinetics in rats and antitumor effect in various types of tumor-bearing mice of novel self-assembled gelatine-oleic acid nanoparticles containing paclitaxel. *J Biomed Nanotechnol* **10**: 154–165. <https://doi.org/10.1166/jbn.2014.1660>
- Tseng CL, Wu SY, Wang WH (2008). Targeting efficiency and bio-distribution of biotinylated-EGF-conjugated gelatin nanoparticles administered *via* aerosol delivery in nude mice with lung cancer. *Biomaterials* **29**: 3014–3022. <https://doi.org/10.1016/j.biomaterials.2008.03.033>
- Yoo MK, Park IK, Lim HT (2012) Folate-PEG-superparamagnetic iron oxide nanoparticles for lung cancer imaging. *Acta Biomaterialia* **8**: 3005–3013. <https://doi.org/10.1016/j.actbio.2012.04.029>
- Zhang X, Gan Y, Gan L, Nie S, Pan W (2008). PEGylated nanostructured lipid carriers loaded with 10 hydroxycamptothecin: an efficient carrier with enhanced anti tumour effects against lung cancer. *J Pharm Pharmacol* **60**: 1077–1087. <https://doi.org/10.1211/jpp.60.8.0014>.